



## Short communication

Li<sub>2</sub>FeSiO<sub>4</sub>/C cathode material synthesized by template-assisted sol–gel process with Fe<sub>2</sub>O<sub>3</sub> microsphereLong Qu<sup>a</sup>, Shaohua Fang<sup>a,\*</sup>, Li Yang<sup>a,\*</sup>, Shin-ichi Hirano<sup>b</sup><sup>a</sup>School of Chemistry and Chemical Technology, Shanghai Jiaotong University, Shanghai 200240, China<sup>b</sup>Hirano Institute for Materials Innovation, Shanghai Jiaotong University, Shanghai 200240, China

## H I G H L I G H T S

- ▶ Li<sub>2</sub>FeSiO<sub>4</sub>/C nanocomposite is prepared by sol–gel method with Fe<sub>2</sub>O<sub>3</sub> microsphere.
- ▶ It exhibits sphere-like morphology.
- ▶ It owns stable cycle performance at 0.1 C–2 C rate.

## A R T I C L E I N F O

## Article history:

Received 25 February 2012

Received in revised form

14 May 2012

Accepted 28 May 2012

Available online 13 June 2012

## Keywords:

Lithium-ion battery

Cathode materials

Li<sub>2</sub>FeSiO<sub>4</sub>Fe<sub>2</sub>O<sub>3</sub> microsphere

## A B S T R A C T

Fe<sub>2</sub>O<sub>3</sub> microsphere is used as iron source and template to prepare Li<sub>2</sub>FeSiO<sub>4</sub>/C nanocomposite by a sol–gel method. The carbon content, structure, and morphology of the sample are characterized by carbon–sulfur inferred analysis (CSI), X-ray diffraction (XRD), scanning electron microscope (SEM), and transmission electron microscopy (TEM) techniques. The results show that the Li<sub>2</sub>FeSiO<sub>4</sub>/C owns pure phase and sphere-like morphology as a result of an agglomeration of nanoparticles with an average particle size of about 50 nm. The Li<sub>2</sub>FeSiO<sub>4</sub>/C exhibits stable cycle performance at different rates from 0.1 C to 2 C, and its capacity at 0.1 C rate can reach 160 mAh g<sup>−1</sup>.

© 2012 Elsevier B.V. All rights reserved.

## 1. Introduction

Lithium-ion batteries have been widely applied on the portable electric power tools and other electronic products, and they are considered as the promising power sources of electric vehicles (EVs) [1]. During the past decade, polyanion-type compounds containing (XO<sub>4</sub>)<sup>n−</sup> group as the cathode materials of lithium-ion batteries have attracted much attention because of their low exothermicity and high safety, compared with lithium transition-metal oxides, such as LiMn<sub>2</sub>O<sub>4</sub>, LiCoO<sub>2</sub>, and Li[Ni,Co,Mn]O<sub>2</sub> [2,3]. Among the polyanion compounds, lithium transition-metal orthosilicate (Li<sub>2</sub>MSiO<sub>4</sub>, M = Fe, Mn, etc.) own the higher theoretical capacity (2 mol of Li<sup>+</sup> per formula unit) [4–8]. Recently, more and more researchers focus on Li<sub>2</sub>FeSiO<sub>4</sub>, due to its excellent cycle performance [9–25]. In addition, Li<sub>2</sub>FeSiO<sub>4</sub> is inexpensive,

nonpoisonous, and environmental friendly, because the elements of O, Si, and Fe are contained most abundantly on the earth.

However, Li<sub>2</sub>FeSiO<sub>4</sub> suffers from the problem of poor electronic conductivity and slow diffusion rate of lithium ion [10,26], which prevent it from further applications. It is reported that preparing carbon-coated Li<sub>2</sub>FeSiO<sub>4</sub> composite (Li<sub>2</sub>FeSiO<sub>4</sub>/C) and decreasing particle size to nano-scale are two effective approaches to overcome these obstacles [27,28]. Up to now, great efforts have been offered to prepare Li<sub>2</sub>FeSiO<sub>4</sub>/C as the cathode material for lithium-ion battery by different synthetic methods [6,7,9–25]. Solid-state reaction method is appropriate to the large-scale production, but the impurities and the larger particle size of the product could not be avoidable, due to the prolonged heat treatment at a high temperature [6,20,22,23]. Direct hydrothermal method is difficult to acquire Li<sub>2</sub>FeSiO<sub>4</sub> or Li<sub>2</sub>FeSiO<sub>4</sub>/C with pure phase, and the products own low crystallinity, which make negative effects on the electrochemical performances of the products, although this approach can reduce the particle size [7,9,25]. Sol–gel method can greatly improve the homogeneity of the precursor, and the as-

\* Corresponding authors. Tel.: +86 21 54748917; fax: +86 21 54741297.

E-mail addresses: [housefang@sjtu.edu.cn](mailto:housefang@sjtu.edu.cn) (S. Fang), [liyange@sjtu.edu.cn](mailto:liyange@sjtu.edu.cn) (L. Yang).

prepared  $\text{Li}_2\text{FeSiO}_4/\text{C}$  exhibits pure phase, nano-scale particle size, and excellent electrochemical performance. For example, Dominko et al. have firstly synthesized  $\text{Li}_2\text{FeSiO}_4/\text{C}$  composite basing on sol–gel reflux method, by using the soluble  $\text{Fe}(\text{NO}_3)_3$ , or  $\text{FeC}_6\text{H}_5\text{O}_7$  (ferric citrate) as Fe source and the insoluble nano- $\text{SiO}_2$  as Si source [9]. If the nano- $\text{SiO}_2$  is replaced by the soluble silicane, such as tetraethyl orthosilicate (TEOS), the molecular-level mixing of Li, Fe and Si elements can be achieved during the process of forming sol–gel. Representatively, the  $\text{Li}_2\text{FeSiO}_4/\text{C}$  nanocomposites have been prepared by the microwave-solvothermal and hydrothermal-assisted sol–gel methods, and the products show better performance [11,14]. Furthermore, the *in-situ* generated carbon can help to restrict the increasing of the  $\text{Li}_2\text{FeSiO}_4$  particle size during the heat treatment. Through modifying the carbon coating techniques, the electrochemical properties of  $\text{Li}_2\text{FeSiO}_4$  could also be improved. Recently, porous  $\text{Li}_2\text{FeSiO}_4/\text{C}$  have been prepared by introducing carbon source during sol–gel process, and more than 1 mol of  $\text{Li}^+$  per formula unit can be extracted from the porous  $\text{Li}_2\text{FeSiO}_4/\text{C}$  [16,17].

Usually, the main impurities in the  $\text{Li}_2\text{FeSiO}_4/\text{C}$  are iron oxides and lithium silicates in the previous investigations, which are looked on as the infaust factors to electrochemical performance [7,20]. Is it possible to replace iron salts by iron oxides to prepare pure-phased  $\text{Li}_2\text{FeSiO}_4/\text{C}$  via simple processes? This assumption had been proved to be feasible in this work.  $\text{Fe}_2\text{O}_3$  microsphere is used as the Fe source and template to synthesize the sphere-like  $\text{Li}_2\text{FeSiO}_4/\text{C}$  nanocomposite by sol–gel method. Furthermore, the  $\text{Li}_2\text{FeSiO}_4/\text{C}$  nanocomposite exhibits stable cycle performance at different rates from 0.1 C to 2 C.

## 2. Experimental

### 2.1. Preparation of $\text{Fe}_2\text{O}_3$ microsphere

All the reagents and solvents were analytical purity, and purchased from Sinopharm Chemical Reagent Co. Ltd., and used as received.  $\text{Fe}_3\text{O}_4$  microsphere was synthesized by hydrothermal method as described in the literature [29]. In order to remove the absorbed surfactants,  $\text{Fe}_3\text{O}_4$  microsphere was heated at 400 °C for 2 h under atmosphere to obtain  $\text{Fe}_2\text{O}_3$  microsphere.

### 2.2. Preparation of $\text{Li}_2\text{FeSiO}_4/\text{C}$ composites

The  $\text{Li}_2\text{FeSiO}_4/\text{C}$  composite was synthesized by sol–gel method. Typically, the stoichiometric amounts of  $\text{LiCH}_3\text{COO} \cdot 2\text{H}_2\text{O}$  (0.02 mol), as-prepared  $\text{Fe}_2\text{O}_3$  microsphere (0.005 mol), and TEOS (0.01 mol) were dispersed in water–ethanol (1:10 V/V) and  $\text{CH}_3\text{COOH}$  was added as a catalyst. The mixture were stirred by mechanical stirring and refluxed at 85 °C for at least 24 h. Then the solvents were evaporated slowly at 100 °C under continuous stirring until the brown gel was formed. After being dried at 100 °C for 10 h, the power was fine grinded by ball-milling with sucrose and acetone at least for 8 h. After evaporating the acetone, the dry powder was calcinated in a horizontal quartz tube oven at 700 °C for 10 h at argon atmosphere to obtain the  $\text{Li}_2\text{FeSiO}_4/\text{C}$  composite.

### 2.3. Materials characterization

The structures of  $\text{Fe}_2\text{O}_3$  and  $\text{Li}_2\text{FeSiO}_4/\text{C}$  composite were determined by X-ray diffraction (XRD, Rigaku, D/max-2200 PC) with  $\text{Cu K}\alpha$  radiation operated at 40 kV and 20 mA. The morphologies of  $\text{Fe}_2\text{O}_3$  and  $\text{Li}_2\text{FeSiO}_4/\text{C}$  composite were observed by using a field-emission scanning electron microscope (FE-SEM, NOVA NanoSEM 230) and a high-resolution transmission electron microscope (HR-TEM, JEM-2010HT). The amount of carbon in  $\text{Li}_2\text{FeSiO}_4/\text{C}$

composite was 16 wt% measured by using a high frequency carbon–sulfur infrared analyzer (CSI, Shanghai Baoying Photoelectric Technology Co. Ltd., CS-206).

### 2.4. Electrode preparation and electrochemical measurements

The electrochemical performances of  $\text{Li}_2\text{FeSiO}_4/\text{C}$  composites were assessed using CR-2016 coin cells. The cathode was prepared by mixing 80 wt% of  $\text{Li}_2\text{FeSiO}_4/\text{C}$  composites with 10 wt% carbon black and 10 wt% poly(vinylidene fluoride) (PVDF) dissolved in *N*-methyl-2-pyrrolidone (NMP). All reported capacity values were quoted with respect to the mass of the  $\text{Li}_2\text{FeSiO}_4$ . The electrodes were formed by coating the slurry onto Al foils after drying overnight at 110 °C in a vacuum oven, and the typical cathode loading was 1–2  $\text{mg cm}^{-2}$ . The cells were assembled with the cathode as prepared, with Li metal as the anode, and with glass fiber (Whatman GF/A) as the separator. The electrolytes were 1 M  $\text{LiPF}_6$  dissolved in ethylene carbonate/dimethyl carbonate (1:1 w/w). Cell assembling was carried out in a glove-box (Braun, Master 100 Lab) full-filled with argon atmosphere. Galvanostatic charge–discharge measurements were executed between 1.5 and 4.8 V at room temperature by a Land CT 2001 battery test system, and 1 C rate was corresponding to current density of 160  $\text{mAh g}^{-1}$ . Because of the sensitivity of the material in air, materials characterization and cells assembling were completed in a week after the materials preparation.

## 3. Results and discussions

The structures of iron oxide and  $\text{Li}_2\text{FeSiO}_4/\text{C}$  composite are determined by XRD. It can be easily found from Fig. 1a that the pattern is indexed to  $\text{Fe}_2\text{O}_3$  (JCPDS 25-1402), which indicates that the Fe source applied on the experiment is  $\text{Fe}_2\text{O}_3$ . As shown in Fig. 1b, the diffraction peaks of  $\text{Li}_2\text{FeSiO}_4/\text{C}$  composite are in full accord with the  $\text{Li}_2\text{FeSiO}_4$  structure indexed by orthorhombic  $Pmn2_1$  [6,30,31]. The diffraction peaks of the carbon coating are not observed in the XRD pattern due to its amorphous state. It is interesting that no iron oxides, lithium silicates, and other impurities phases are observed for the resulting product. In previous reports, the reductive atmospheres were often used to suppress the formation of iron oxides impurities [6,9,24]. In our preparation,

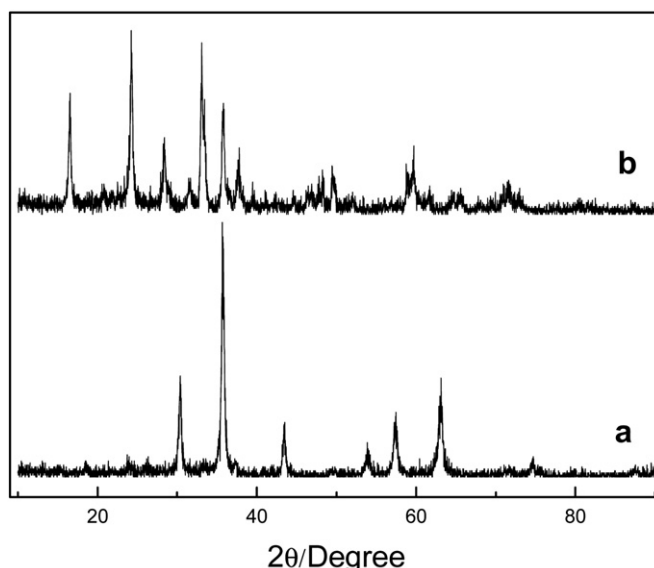


Fig. 1. XRD patterns of (a)  $\text{Fe}_2\text{O}_3$  and (b)  $\text{Li}_2\text{FeSiO}_4/\text{C}$ .

carbon is the only reducer, which is generated from the carbonization of sucrose during the calcination process. It suggests that the  $\text{Fe}_2\text{O}_3$  particles react with Li and Si sources under the reduction of carbon to produce the  $\text{Li}_2\text{FeSiO}_4$  during the calcination process, and the presence of carbon has no effect on the development of  $\text{Li}_2\text{FeSiO}_4$  phase. In a word, the result of XRD measurement indicates that the  $\text{Li}_2\text{FeSiO}_4/\text{C}$  composite prepared by sol–gel method with  $\text{Fe}_2\text{O}_3$  shows the pure phase.

The morphologies of  $\text{Fe}_2\text{O}_3$  and  $\text{Li}_2\text{FeSiO}_4/\text{C}$  composite are examined by FE-SEM and HR-TEM. Fig. 2a–d shows the SEM images of  $\text{Fe}_2\text{O}_3$  and  $\text{Li}_2\text{FeSiO}_4/\text{C}$  composite. It can be seen in Fig. 2a that the  $\text{Fe}_2\text{O}_3$  microspheres exhibit the regularly sphere shape with an average particle diameter of approximately 500 nm. According to the magnified SEM image shown in Fig. 2b, it is obvious that the microsphere is a result of an agglomeration of the smaller nanoparticles. To guarantee the homogeneity of dry gel, the monodisperse  $\text{Fe}_2\text{O}_3$  microsphere is pursued in this preparation. Interestingly, as shown in the SEM images of  $\text{Li}_2\text{FeSiO}_4/\text{C}$  composite (Fig. 2c and d), some sphere-like particles with the bumped surface, which is attributed to the carbon coating probably, can be observed easily, and the average particle diameter is close to the  $\text{Fe}_2\text{O}_3$  microsphere's. TEM measurement is used to further investigate the particle size of  $\text{Li}_2\text{FeSiO}_4/\text{C}$  composite and the carbon coating, and the images are shown in Fig. 3a–c. Some sphere-like particles of  $\text{Li}_2\text{FeSiO}_4/\text{C}$  composite can be found from Fig. 3a. According to the magnified TEM image shown in Fig. 3b, the  $\text{Li}_2\text{FeSiO}_4/\text{C}$  composite is also a result of an agglomeration of the nanoparticles with an

average particle size of approximately 50 nm, which is similar to the SEM result of  $\text{Fe}_2\text{O}_3$  (Fig. 2a and b). The HR-TEM image in Fig. 3c reveals that the  $\text{Li}_2\text{FeSiO}_4$  nanocrystals are wrapped by the amorphous carbon coating with the thick of several nanometers, although the boundary of them is obscure. Generally, these results indicate that the  $\text{Fe}_2\text{O}_3$  microsphere can be pursued as the template to prepare the  $\text{Li}_2\text{FeSiO}_4/\text{C}$  nanocomposite with the sphere-like morphology.

Galvanostatic charge–discharge measurements are carried out to assess the electrochemical performances of  $\text{Li}_2\text{FeSiO}_4/\text{C}$  nanocomposite cathode. Fig. 4 shows the charge–discharge profiles at 0.1 C rate for different cycles. It can be found that the 2nd charge plateau is obviously lower than the initial one, however its discharge plateau is similar to the initial one, which suggests that a Li/Fe disordering process might occur during first charge [32]. The  $\text{Li}_2\text{FeSiO}_4/\text{C}$  nanocomposite delivers an initial discharge capacity of about  $140 \text{ mAh g}^{-1}$ , and the discharge capacity increases gradually with the increasing cycle number. The charge–discharge profiles of 10th and 15th cycles almost overlap the 5th one, which implies that the crystal structure is stable and there is no major structural change occurred after 5 cycles [33].

To investigate the cycle performance of the  $\text{Li}_2\text{FeSiO}_4/\text{C}$  nanocomposite, it is tested for 100 cycles at different rates, and the results are shown in Fig. 5. For the performance cycled at 0.1 C rate, after the discharge capacity increases during the initial several cycles, it is stable at about  $160 \text{ mAh g}^{-1}$  until the 50th cycle, which is about 96% of the theoretical capacity extracted 1 mol of  $\text{Li}^+$  per

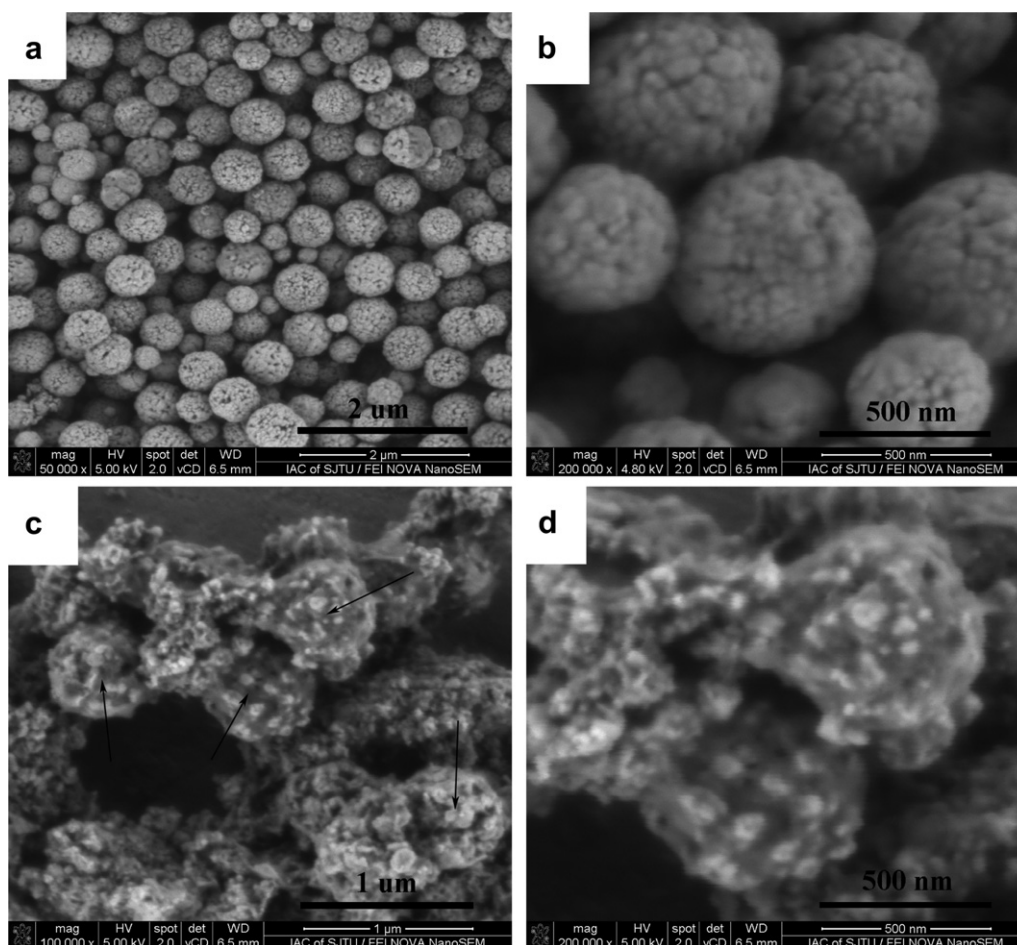
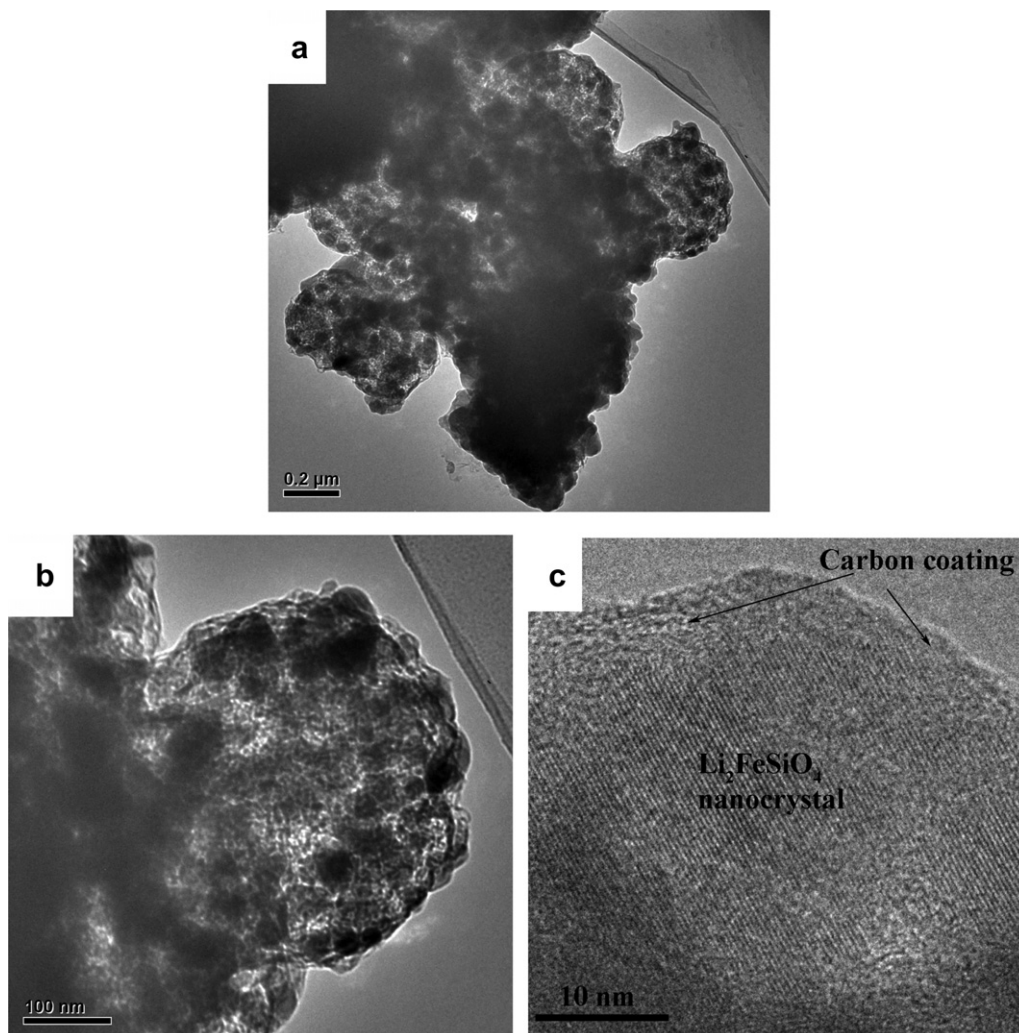


Fig. 2. SEM images of  $\text{Fe}_2\text{O}_3$  microsphere at (a) low and (b) high magnification, and  $\text{Li}_2\text{FeSiO}_4/\text{C}$  nanocomposites at (c) low and (d) high magnification.



**Fig. 3.** TEM images of  $\text{Li}_2\text{FeSiO}_4/\text{C}$  nanocomposite at (a) low and (b) high magnification, and (c) HR-TEM image of  $\text{Li}_2\text{FeSiO}_4/\text{C}$  nanocomposite.

formula unit ( $166 \text{ mAh g}^{-1}$ ), then it slowly decreases with the increasing cycle number. Nevertheless, the discharge capacity is about  $146 \text{ mAh g}^{-1}$  in the 100th cycle, and about 91% of the maximum value is still retained. Apparently, the capacity decreases

with the increasing of rate. For 0.2 C, 0.5 C, 1 C, and 2 C rate, the capacities also increase with the increasing cycle number during the initial some cycles, and they are stable at about  $140 \text{ mAh g}^{-1}$ ,  $115 \text{ mAh g}^{-1}$ ,  $105 \text{ mAh g}^{-1}$ , and  $95 \text{ mAh g}^{-1}$  until the 100th cycle,

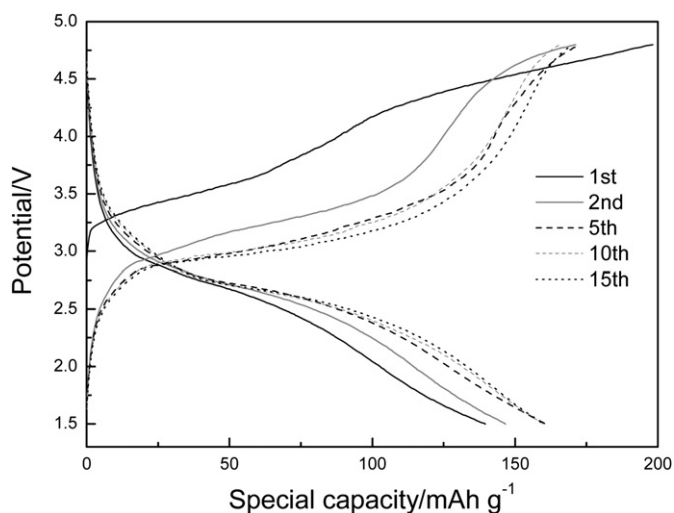


**Fig. 4.** Charge–discharge curves of  $\text{Li}_2\text{FeSiO}_4/\text{C}$  nanocomposite cycled at 0.1 C rate.

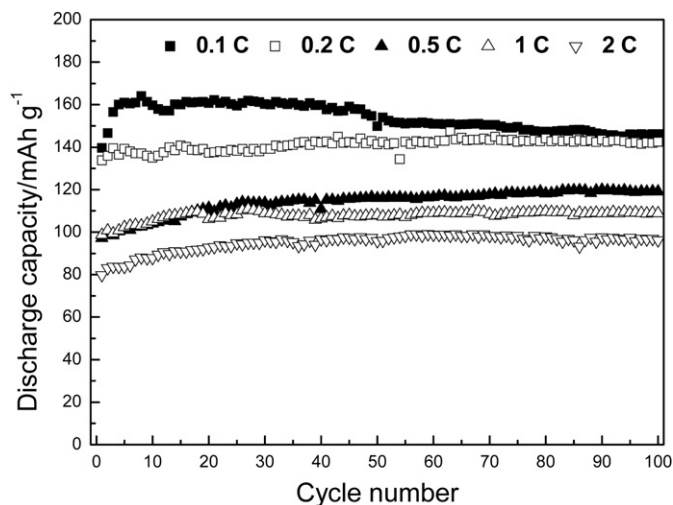


**Fig. 5.** The discharge capacities and cycle performances of  $\text{Li}_2\text{FeSiO}_4/\text{C}$  nanocomposite cycled at 0.1 C, 0.2 C, 0.5 C, 1 C, and 2 C rate.



respectively. Hitherto, in the potential range of 1.5–4.8 V, few researches about the cycle performance more than 50 times at 0.1 C or lower rate have been reported [12,19]. When the cell is tested at 0.1 C or lower rate, the charging process could be maintained for a long time in the high potential, where the side reactions between electrode and electrolyte are intensive. In order to obtain the stable cycle performance at the low rate in the wide potential range, the quality of carbon coating should be improved to restrain those side reactions. In this work, the  $\text{Li}_2\text{FeSiO}_4/\text{C}$  nanocomposite exhibits excellent cycle performance at different rates from 0.1 C to 2 C during 100 cycles, which implies that the carbon coating can prevent  $\text{Li}_2\text{FeSiO}_4$  effectively from reacting with the  $\text{PF}_5$  or HF from the  $\text{LiPF}_6$  salt in the organic electrolyte [34]. The  $\text{Li}_2\text{FeSiO}_4/\text{C}$  nanocomposite has not exhibited higher capacity performance under the high-rate condition, and it could be attributed to its larger particle size of the active material. In the further investigation, we expect to synthesize  $\text{Li}_2\text{FeSiO}_4/\text{C}$  by using  $\text{Fe}_2\text{O}_3$  with smaller particle size.

#### 4. Conclusions

In summary,  $\text{Li}_2\text{FeSiO}_4/\text{C}$  nanocomposite has been synthesized as cathode material of lithium-ion battery by a template-assisted sol–gel method with  $\text{Fe}_2\text{O}_3$  microsphere. It is found that the sample owns pure phase, sphere-like morphology, and nano-structure. The  $\text{Li}_2\text{FeSiO}_4/\text{C}$  exhibits stable cycle performance at different rates from 0.1 C to 2 C, and it delivers a high capacity of 160 mAh  $\text{g}^{-1}$  at 0.1 C rate in the 5th cycle and retains capacity of 146 mAh  $\text{g}^{-1}$  in the 100th cycle.

#### Acknowledgments

The financial supports from the National Natural Science Foundation of China (Grants No. 21173148 and 21103108) are gratefully acknowledged. We thank the Instrumental Analysis Center of Shanghai Jiao Tong University for Materials Characterization.

#### References

- [1] J.M. Tarascon, M. Armand, *Nature* 414 (2001) 359–367.
- [2] M.S. Whittingham, *Chemical Reviews* 104 (2004) 4271–4301.
- [3] J.W. Fergus, *Journal of Power Sources* 195 (2010) 939–954.
- [4] A.K. Padhi, K.S. Nanjundaswamy, J.B. Goodenough, *Journal of the Electrochemical Society* 144 (1997) 1188–1194.
- [5] A. Yamada, M. Hosoya, S.C. Chung, Y. Kudo, K. Hinokuma, K.Y. Liu, Y. Nishi, *Journal of Power Sources* 119–121 (2003) 232–238.
- [6] A. Nyttén, A. Abouimrane, M. Armand, T. Gustafsson, J.O. Thomas, *Electrochemistry Communications* 7 (2005) 156–160.
- [7] R. Dominko, M. Bele, M. Gaberscek, A. Meden, M. Remskar, J. Jamnik, *Electrochemistry Communications* 8 (2006) 217–222.
- [8] Y.-X. Li, Z.-L. Gong, Y. Yang, *Journal of Power Sources* 174 (2007) 528–532.
- [9] R. Dominko, D.E. Conte, D. Hanzel, M. Gaberscek, J. Jamnik, *Journal of Power Sources* 178 (2008) 842–847.
- [10] R. Dominko, *Journal of Power Sources* 184 (2008) 462–468.
- [11] Z.L. Gong, Y.X. Li, G.N. He, J. Li, Y. Yang, *Electrochemical and Solid State Letters* 11 (2008) A60–A63.
- [12] S. Zhang, C. Deng, S. Yang, *Electrochemical and Solid State Letters* 12 (2009) A136–A139.
- [13] C. Deng, S. Zhang, B.L. Fu, S.Y. Yang, L. Ma, *Materials Chemistry and Physics* 120 (2010) 14–17.
- [14] T. Muraliganth, K.R. Stroukoff, A. Manthiram, *Chemistry of Materials* 22 (2010) 5754–5761.
- [15] X.Y. Fan, Y. Li, J.J. Wang, L. Gou, P. Zhao, D.L. Li, L. Huang, S.G. Sun, *Journal of Alloys and Compounds* 493 (2010) 77–80.
- [16] D. Lv, W. Wen, X. Huang, J. Bai, J. Mi, S. Wu, Y. Yang, *Journal of Materials Chemistry* 21 (2011) 9506–9512.
- [17] Z. Zheng, Y. Wang, A. Zhang, T. Zhang, F. Cheng, Z. Tao, J. Chen, *Journal of Power Sources* 198 (2012) 229–235.
- [18] Z. Yan, S. Cai, L. Miao, X. Zhou, Y. Zhao, *Journal of Alloys and Compounds* 511 (2012) 101–106.
- [19] B. Shao, I. Taniguchi, *Journal of Power Sources* 199 (2012) 278–286.
- [20] K.C. Kam, T. Gustafsson, J.O. Thomas, *Solid State Ionics* 192 (2011) 356–359.
- [21] H.J. Guo, K.X. Xiang, X. Cao, X.H. Li, Z.X. Wang, L.M. Li, *Transactions of Nonferrous Metals Society of China (English Edition)* 19 (2009) 166–169.
- [22] Z. Dong Peng, Y. Bing Cao, G. Rong Hu, K. Du, X. Guang Gao, Z. Wei Xiao, *Chinese Chemical Letters* 20 (2009) 1000–1004.
- [23] X. Huang, X. Li, H. Wang, Z. Pan, M. Qu, Z. Yu, *Electrochimica Acta* 55 (2010) 7362–7366.
- [24] T. Kojima, A. Kojima, T. Miyuki, Y. Okuyama, T. Sakai, *Journal of the Electrochemical Society* 158 (2011) A1340–A1346.
- [25] M. Zhang, Q. Chen, Z. Xi, Y. Hou, *Journal of Materials Science* (2011) 1–5.
- [26] S.-Y. Chung, J.T. Bloking, Y.-M. Chiang, *Nature Materials* 1 (2002) 123–128.
- [27] A. Yamada, S.C. Chung, K. Hinokuma, *Journal of the Electrochemical Society* 148 (2001) A224–A229.
- [28] H. Huang, S.C. Yin, L.F. Nazar, *Electrochemical and Solid State Letters* 4 (2001) A170–A172.
- [29] H. Deng, X. Li, Q. Peng, X. Wang, J. Chen, Y. Li, *Angewandte Chemie International Edition* 44 (2005) 2782–2785.
- [30] K. Zaghib, A. Ait Salah, N. Ravet, A. Mauger, F. Gendron, C.M. Julien, *Journal of Power Sources* 160 (2006) 1381–1386.
- [31] C. Keffer, A.D. Mighell, F. Mauer, H.E. Swanson, S. Block, *Inorganic Chemistry* 6 (1967) 119–125.
- [32] A. Nyttén, S. Kamali, L. Häggström, T. Gustafsson, J.O. Thomas, *Journal of Materials Chemistry* 16 (2006) 2266–2272.
- [33] C. Sirisopanaporn, C. Masquelier, P.G. Bruce, A.R. Armstrong, R. Dominko, *Journal of the American Chemical Society* 133 (2011) 1263–1265.
- [34] A. Nyttén, M. Stjerndahl, H. Rensmo, H. Siegbahn, M. Armand, T. Gustafsson, K. Edström, J.O. Thomas, *Journal of Materials Chemistry* 16 (2006) 3483–3488.